

Sequential pattern load modeling and warning-system plan in modular falsework

Jui-Lin Peng†

*Department of Construction Engineering, Yunlin University of Science and Technology,
Yunlin, 640, Taiwan, R.O.C.*

Cheng-Lung Wu‡

Department of Construction Engineering, Chaoyang University of Technology, Taichung, 413, Taiwan, R.O.C.

Siu-Lai Chan‡†

Department of Civil and Structural Engineering, Hong Kong Polytechnic University, Hong Kong, China

(Received December 3, 2002, Accepted July 7, 2003)

Abstract. This paper investigates the structural behavior of modular falsework system under sequential pattern loads. Based on the studies of 25 construction sites, the pattern load sequence modeling is defined as models R (rectangle), L and U . The study focuses on the system critical loads, regions of largest reaction forces, discrepancy between the pattern load and the uniform load, and the warning-system plan. The analysis results show that the critical loads of modular falsework systems with sequential pattern loads are very close to those with the uniform load used in design. The regions of largest reaction forces are smaller than those calculated by the uniform load. However, the regions of largest reaction forces of three models under sequential pattern loads can be considered as the crucial positions of warning-system based on the measured index of loading. The positions of the sensors for the warning-system for these three different models are not identical.

Key words: critical load; modular falsework; pattern load; load path; warning-system.

1. Introduction

From a survey of construction accidents (Hadipriono and Wang 1986, Council 1997), most falsework collapses occur during the placing of fresh concrete. The weight of fresh concrete is the largest part of construction loads, which also include steel, formwork, crew, etc. It has been suspected that certain characteristics of fresh concrete induce falsework collapse. Prior research on falsework has focused on the load-carrying capacity of the resistance part, such as modular

† Associate Professor

‡ Graduate Student

‡† Professor

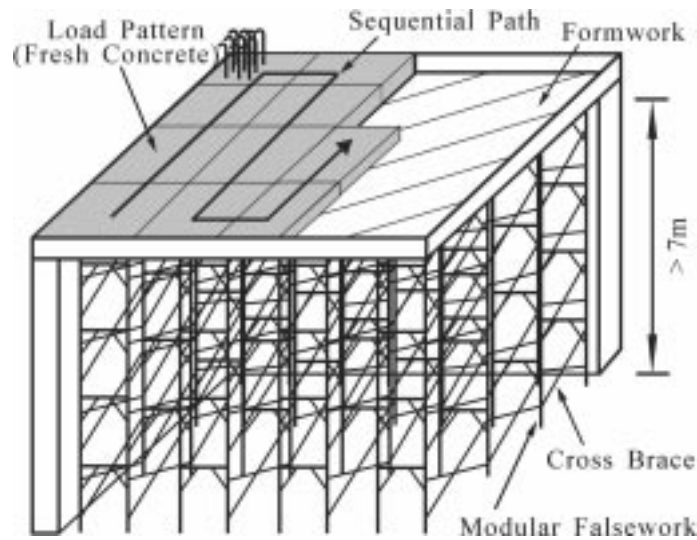


Fig. 1 Sequential pattern load on modular falsework system

falsework systems (Huang *et al.* 2000, Peng *et al.* 1996a & 1996b). Almost no research has been undertaken on the topic of loading incurred during construction.

Most current design codes focus on the safety of buildings during their “service stage.” These codes include explicit specifications for design loads, including maximum wind load, maximum earthquake load, etc. In contrast, little is known about load characteristics of the falsework during construction. The sequential load pattern is the specific characteristic of the fresh concrete placed on formwork during construction. Fig. 1 shows a typical sequential pattern load of fresh concrete placed on a modular falsework system. According to recent surveys (Yen *et al.* 2000), the weight of fresh concrete is the largest portion of the external load on formwork. However, existing design specifications offer only limited provisions to account for the pattern loads and the effect of the load placement during the “construction stage.” Previous studies on load patterns (Jirsa *et al.* 1969, Jofriet and McNeice 1971) have focused on the structural behavior of slabs under service loads, i.e., evaluating maximum bending moment at a specific position on the slab. The formwork loads in construction was modeled by Rosowsky (Rosowsky *et al.* 1994a & 1994b). The reaction forces of some shores were measured by load cells in tests; those of other shores were calculated by interpolation in his study. However, the extent to which sequential load patterns affect temporary structures and formwork during construction has seldom been addressed.

During construction stage, temporary structures are used to support fresh concrete, construction equipment, materials and workers. Temporary structures are often treated as non-structural frameworks, and they are considered as outside the scope of most codes. For a reinforced concrete building with high headroom, the modular falsework system is typically used as temporary structure during construction. Since the height of formwork used on modular falsework systems is usually above 7 meters, the collapse of this kind of falsework can involve a huge loss of life and property. It is worth finding the possible collapse causes induced by the sequential pattern loads of fresh concrete for falsework systems.

2. Research significance

The present study focuses on the structural behavior of modular falsework systems under sequential pattern loads of fresh concrete. An outdoor large full-scale loading test (Peng *et al.* 1997) is used to compare the analysis result and analysis parameters are refined accordingly. Based on these parameters, the analysis is reliably formulated in this paper. There are three areas investigated as follows.

2.1 Relationship between sequential pattern load and uniform load in design

A temporary structure generally has different types of pattern load sequences of fresh concrete in construction. These pattern loads are cast on formwork sequentially. Calculating the system critical load of the entire modular falsework under pattern load sequences is totally different from that by applying simple uniform load on the temporary falsework.

The uniform load is typically assumed by engineers in design. If the critical load based on the sequential pattern loads is lower than that from uniform load, the collapse load factor of the modular falsework is reduced. However, a simple uniform load is a substitute for the complicate sequential pattern loads in traditional design. It is considered worthy to study and quantify the discrepancy between the uniform load and the sequential pattern load. If the difference is not considerable, the uniform load can replace the complicated sequential pattern load to simplify the design work.

2.2 Region of largest reaction forces of falsework under different pattern load sequences

In general, modular falsework systems have two types of collapses. (1) Direct failure: The external load is larger than the real system critical load of the entire modular falsework system. This leads to the collapse of the whole system. (2) Indirect failure: Some local regions of the modular falsework system fail first which causes the entire system to collapse sequentially. This failure pattern is sometimes referred as progressive collapse.

The second collapse type, indirect failure, may be induced by the *Influence Surface Effect* (Peng *et al.* 1996c). The different pattern load sequences result in an *Influence Surfaces Effect* when the loads are placed on formwork sequentially. In some areas, the reaction forces of the indeterminate falsework system are relatively larger than other places when the system is under sequential load patterns. If the loading lapse time is ignored and only the loading positions are considered, a “largest” reaction force area can be found. Different pattern load sequences may induce various regions of “largest” reaction forces. Thus, the shores in the region of relatively “largest” reaction forces fail first, and then the shores of other positions in the system fail subsequently.

2.3 Warning-system plan based on largest reaction forces

The first consideration in the warning-system plan is the locations of the sensors. Since temporary structures are composed of slender members, the buckling effect is usually considered dominant in the system failure. Thus, the reaction force of the falsework is considered as an index to measure the safety factor of falsework. The horizontal deflection is not appropriate as a measure index since the buckling failure is drastic. The position of the installed warning-system sensor can be considered

for the region of largest reaction forces as in (2) above. The warning-system based on reaction forces can alert workers before the falsework system collapses.

The region of largest reaction forces of falsework is provided in the warning-system plan in the study. The modular falsework system under various pattern load sequences is considered as the first investigated example since the collapse of this type of falsework always makes a larger loss than most other types of falsework.

3. Material properties and formulation

Fig. 2 shows the dimensions of the modular falsework unit used in analysis. The diameter of the cross brace linking two modular falsework units shown in Fig. 1 is also tabulated in the same figure. The Young's modulus E of the modular falsework used in the analysis is 200 Gpa (2.04×10^6 kgf/cm²) and its yield stress F_y is 428 Mpa (4.364×10^3 kgf/cm²).

The numerical calculation is based on a second-order elastic analysis. An equivalent lateral notional force of 0.1-1.0% of total vertical loads is used to simulate the initial imperfections of different modular falsework systems. In the paper, a computer program GMNAF using the pointwise equilibrating polynomial element was developed by Chan (1988), and Chan and Zhou (1994). Compatibility at end nodes and the equilibrium for moment and shear at mid-span are maintained, which eliminates the error associated with conventional displacement-based finite element. The present fifth order element is different from the conventional cubic finite element which requires the use of several elements for second-order analysis.

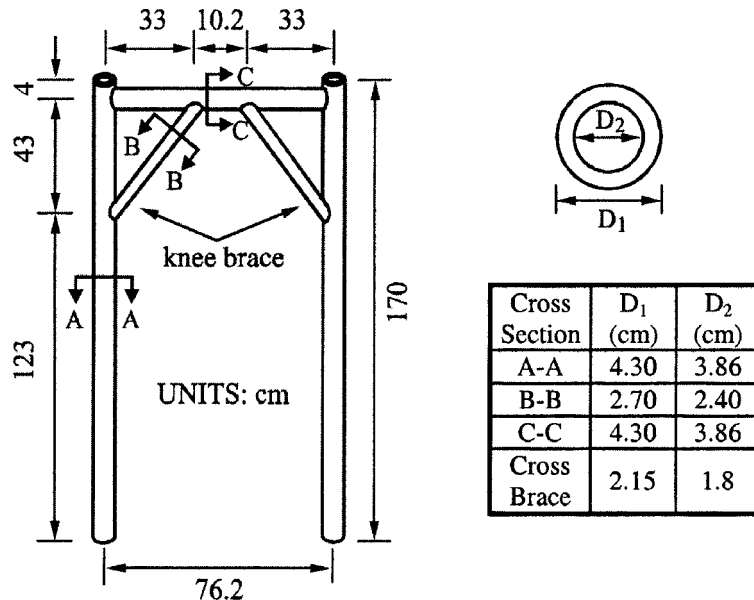


Fig. 2 Dimensions of modular falsework unit

4. Analysis models

4.1 Structural model

The structural models are based on survey studies of 25 concrete buildings in construction sites in Taiwan (Peng *et al.* 2000). Fig. 3 shows three basic models, i.e. models *R* (Rectangle), *L* and *U*. The models are the top plan view of the building types. Models *L* and *U* are continuous and represent the entire system. The direction of arrows shown in the two models in Fig. 3 shows the increase of the side dimension in the analysis. If these two models are not continuous, they are considered as the summation of two or three *R*-models.

The basic *R*-model is a 3-Bay 5-Row 3-Story modular falsework system. The configuration is helpful in comparing the test results of an outdoor large full-scale falsework system (Peng *et al.* 1997). Fig. 4 shows the set-up of the loading test for 3-Bay 5-Row 3-Story modular falsework system. The analyses of models *L* and *U* are also based on this 3-story system in this preliminary study.

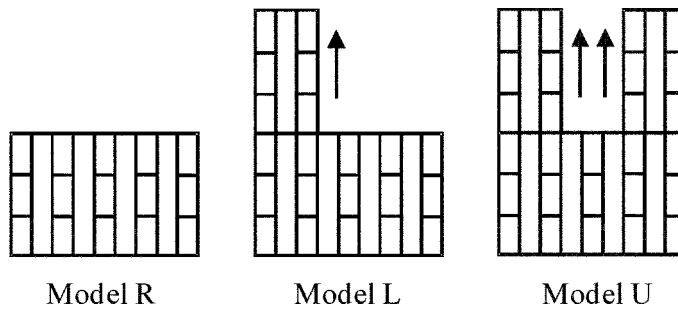


Fig. 3 Models *R*, *L* and *U* of modular falsework systems

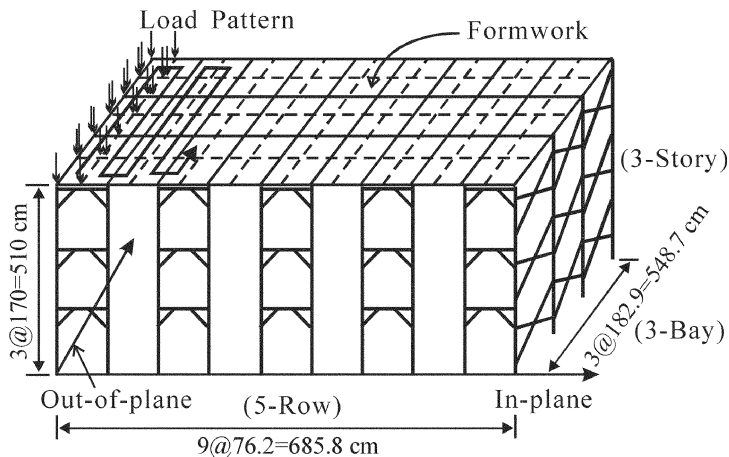


Fig. 4 3-bay 5-row 3-story modular falsework system under sequential pattern load

4.2 Loading model

A sequential pattern load, which is different from the traditional uniform load in design, is shown in Fig. 4. As shown in the figure, a small rectangle with a dashed line on the formwork is the location of each load pattern. The downward arrows on each corner of the rectangle show the pattern loads replacing the uniform loading on the same area. Each load pattern is placed on the four corners of each rectangle block. The folded solid arrow shows the path of the sequential pattern load. All analyses of the three models are based on this pattern load.

5. Experimental comparison

5.1 Regions of largest reaction forces

An outdoor large full-scale loading test of a modular falsework system has been used to verify numerical analyses. Fig. 5 shows this full-scale test using sand bags as the sequential pattern load (Peng *et al.* 1997). The structural behavior of a 3-Bay 5-Row 3-Story modular system was



Fig. 5 Outdoor large full-scale loading test of modular falsework under sequential pattern load

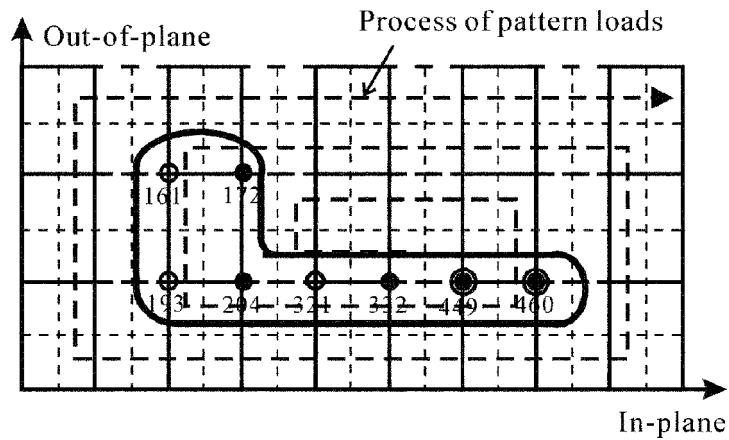


Fig. 8 Comparison of largest reaction forces for case B between test and analysis

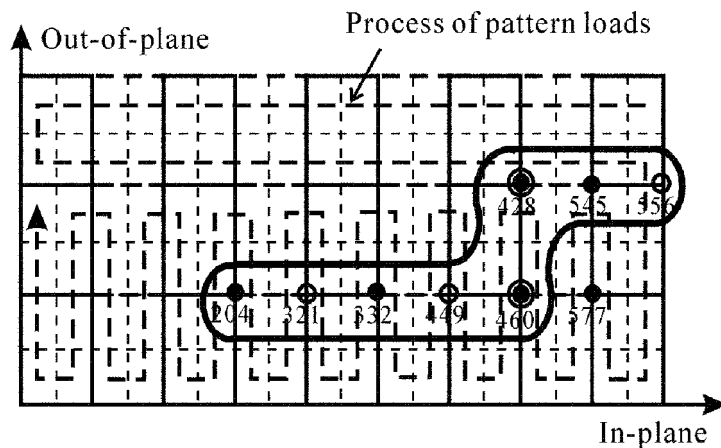


Fig. 9 Comparison of largest reaction forces for case C between test and analysis

5.2 System critical loads

For the outdoor large full-scale loading test of a 3-Bay 5-Row 3-Story modular falsework system, its failure load was 553 kN (56.4 tonnes) under the sequential pattern loads. The analyzed critical load of the entire modular falsework system is 520 kN (53 tonnes) for this sequential pattern load.

In the analysis, the load patterns were placed on the 3-Bay 5-Row 3-Story modular falsework system incrementally. When the total load of the sequential load patterns reached 520 kN, the analysis detects instability. This value, 520 kN, is close to that calculated from the uniform load. After the number of load pattern increases or each load pattern is reduced, the critical loads under sequential pattern load and uniform load are almost identical. Fig. 10 shows the load-deflection curve (P- Δ curve) of the modular falsework system under load path Case A. The trend of this curve under the sequential pattern load is totally different from that calculated from traditional second-order analysis under uniform load.

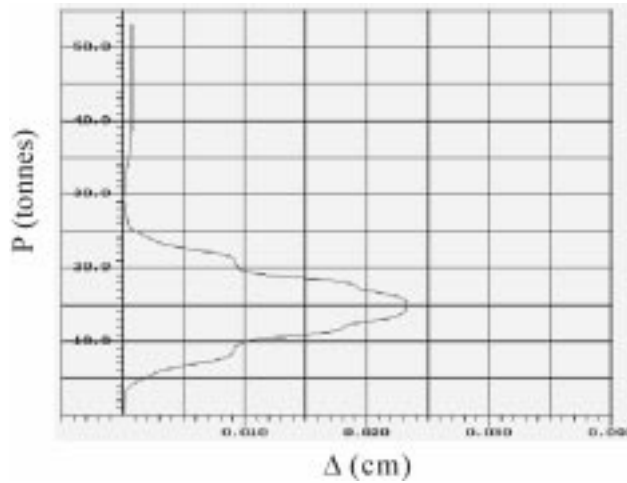


Fig. 10 P - Δ curve of modular falsework system for case A under pattern load

As shown in Figs. 11 and 12, two sequential load patterns were based on survey results from a study of 25 construction sites in Taiwan (Peng *et al.* 2000). In the Figures, the number in the circle represents the sequence of the placed pattern load on the formwork. The critical loads of the two pattern loads are equal to 520 kN (53 tonnes). In addition, the critical load of models L and U with three bays along the extended sides (see Fig. 3) are 657 kN (67 tonnes) and 775 kN (79 tonnes), respectively.

The strength of a system is typically calculated under uniform loading in design. Since the numerical calculation and input is complicated based on the sequential pattern load and the discrepancy of the system critical load between sequential pattern load and uniform load is minimal, the uniform load can be used to replace the sequential pattern load in design.

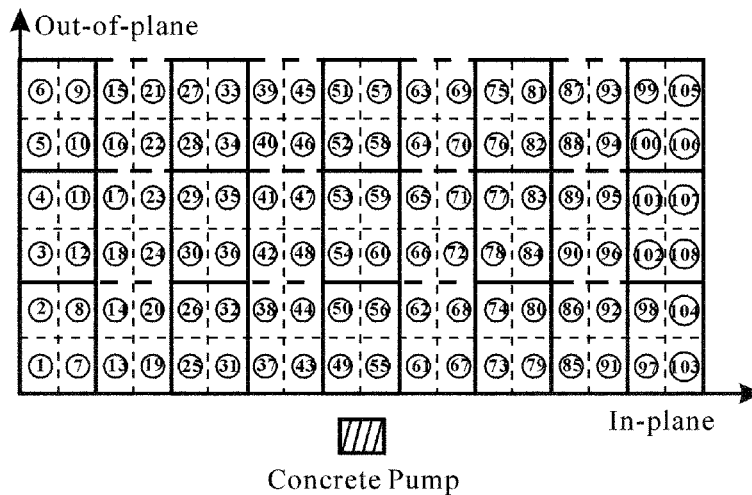


Fig. 11 Load pattern sequence for type (I) of model R measured from construction sites

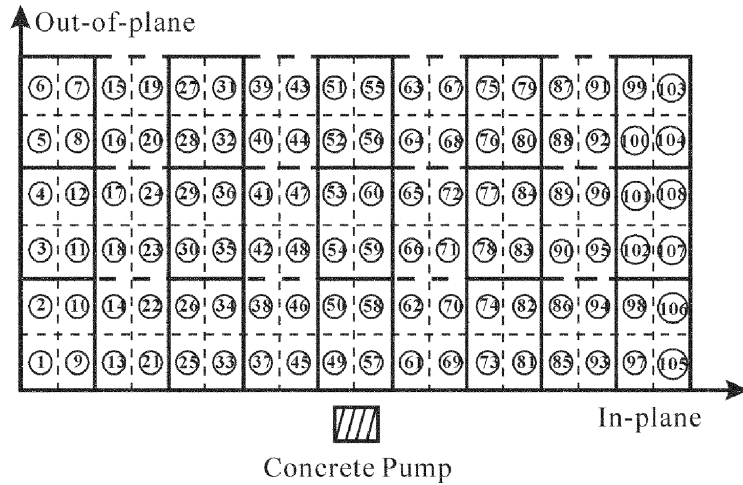


Fig. 12 Load pattern sequence for type (II) of model *R* measured from construction sites

6. Analysis, results and discussion

6.1 Largest reaction forces of modular falsework

6.1.1 Region of largest reaction forces

The largest reaction forces are defined as a specific region having the largest reaction forces of the shores in the modular falsework system irrespective of the occurrence time during the load placing. These largest reaction forces of the modular falsework are induced by the *Influence Surface Effect* in a highly indeterminate structure under loading. This study investigates the positions of largest reaction forces of the falsework shores under each sequential load pattern during the loading process. The prerequisite for this situation is the total loading being less than the system critical load. As a result, the system does not fail directly by the system critical load. The falsework system indirectly fails by some shore failures in a local area due to the *Influence Surface Effect*.

The total load in the analysis is 392 kN (40 tonnes) for model *R*, 628 kN (64 tonnes) for model *L*, and 706 kN (72 tonnes) for model *U*. These values are lower than the system critical loads of 520 kN (53 tonnes) for model *R*, 657 kN (67 tonnes) for model *L*, and 775 kN (79 tonnes) for model *U*. As the total loads of each case are lower than the critical loads, the total loads are suitable for the calculation of the pattern load on the formwork. In the linear response range under moderate load, linear proportionality can be assumed and the following findings can be summarized from the three models.

Model R

Model *R* is based on the survey results from a study of 25 concrete buildings in Taiwan. Figs. 11 and 12 show two sequences of load patterns, types (I) and (II). In the analysis, the total load of model *R* is 392 kN (40 tonnes). The load at each of the four corners is 0.9083 kN (0.009259 tonnes (=40/4/108)) on the small rectangle. If the lapse time of the largest reaction forces is ignored, the largest reaction forces of each pattern load can be found at some specific positions.

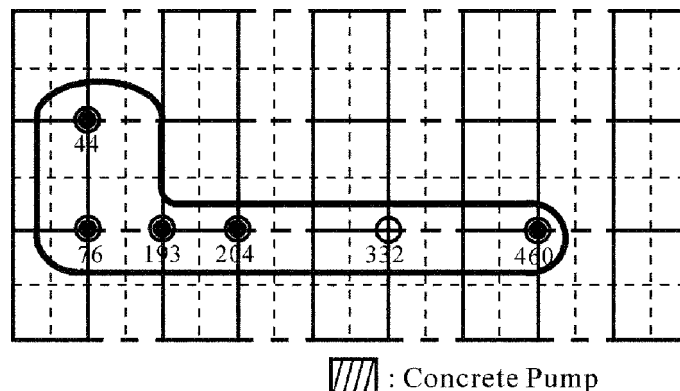


Fig. 13 Comparison of largest reaction forces for types (I) and (II) of model *R*

Fig. 13 shows the comparison of types (I) and (II) under sequential pattern loads for model *R*. In the Figure, the solid symbol “●” reveals the positions of largest reaction forces of the system for type (I) and the hollow symbol “○” for type (II). The result shows that the positions of largest reaction forces are insignificant between these two load types.

In Figs. 7 and 13, the tested result and the analysis can be compared though they have different load sequences. In load placing, the largest reaction forces of two conditions are located at the same nodes, nodes 44, 76, 193 and 204. This means that the measured load sequences are not sensitive to the region of largest reaction forces, of which the region is significant for actual construction practice.

Model *L*

Model *L* is also based on the survey results from a study of 25 concrete buildings in Taiwan. As shown in Figs. 14, 15 and 16, three, six and twelve bays of model *L* are considered in the analysis. The position of concrete pump generally dominates the placing process of the fresh concrete based on the actual survey work in construction. The position of casting fresh concrete commences at the far end of the formwork. After the pattern loads are placed on model *L* based on the sequence of the load patterns, the regions of largest reaction forces can be calculated in Figs. 17, 18 and 19 for three, six and twelve bays respectively.

As shown in Figs. 17, 18 and 19, the solid symbol “●” reveals the positions of largest reaction forces of the three types for model *L*. The values displayed on the arrows show the reaction forces from calculation. The reaction forces indicated in the Figures are the largest values of the whole loading process and limited to the marked locations. These largest reaction forces do not show a big difference during the loading process.

From observing the largest reaction forces of different bays of model *L* in Figs. 17, 18 and 19, it is noted that the largest reaction forces usually locate in similar positions. The region of the largest reaction forces is generally located in the extended bulge part of model *L* and near the left-hand side of the extended bulge part. In addition, the zone ranges from half to top of the extended bulge part of model *L*. If the bay number extends from the bulge part, the region of largest reaction forces is still located in the vicinity of the middle to top parts of the extended bulge. Interestingly, the extended bulge part of model *L* is the commencement of the placing of fresh concrete in construction. If this bulge part is not the first place to cast fresh concrete, the region of largest reaction forces will not be attained in this area.

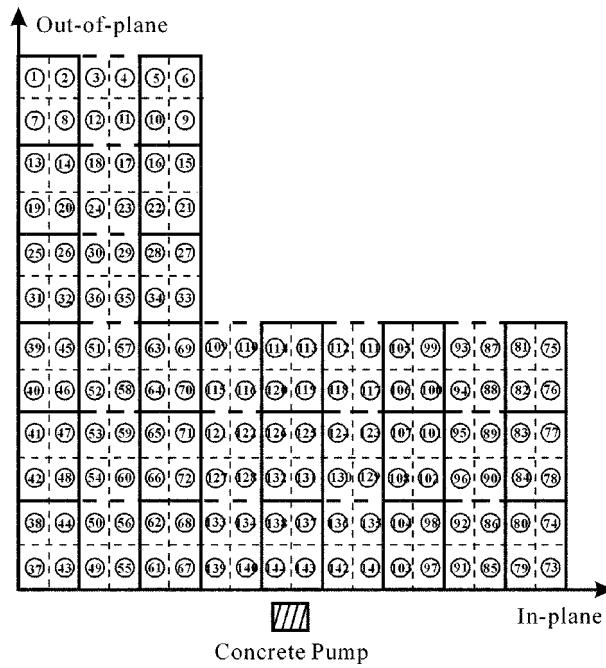


Fig. 14 Load pattern of 3-bay L model based on survey of construction sites

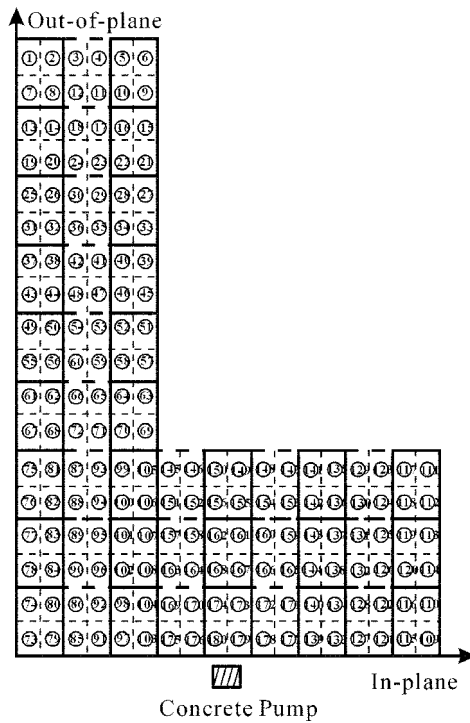


Fig. 15 Load pattern of 6-bay L model based on survey of construction sites

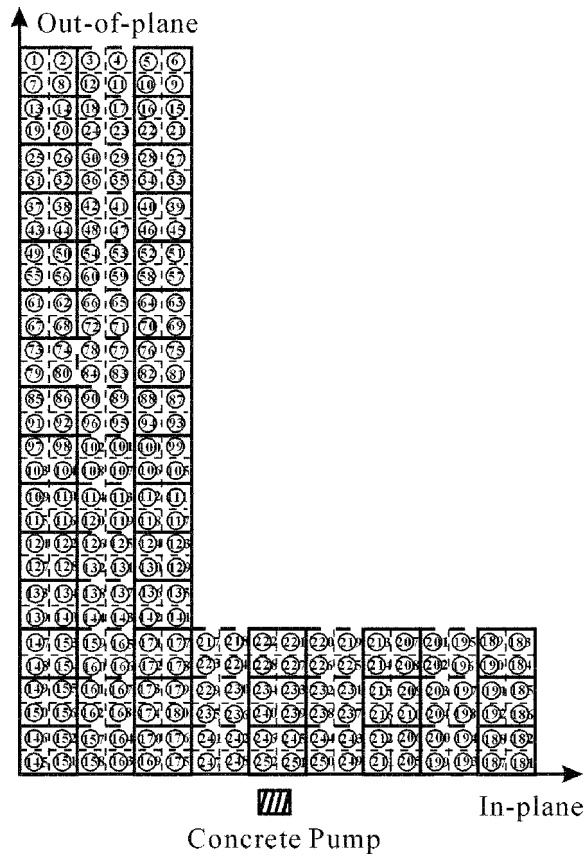


Fig. 16 Load pattern of 12-bay *L* model based on survey of construction sites

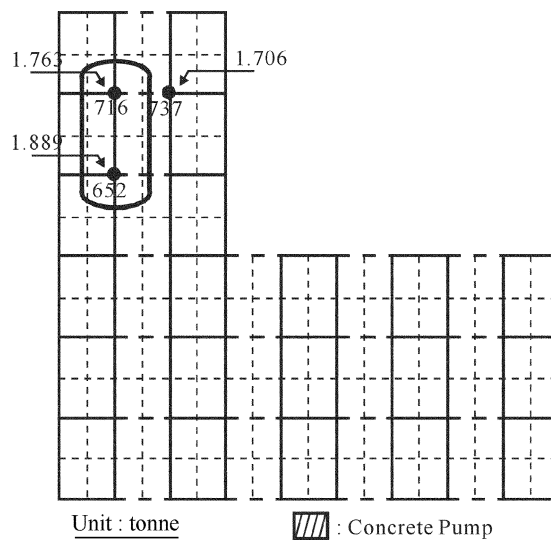


Fig. 17 Largest reaction force area of 3-bay *L* model under pattern load

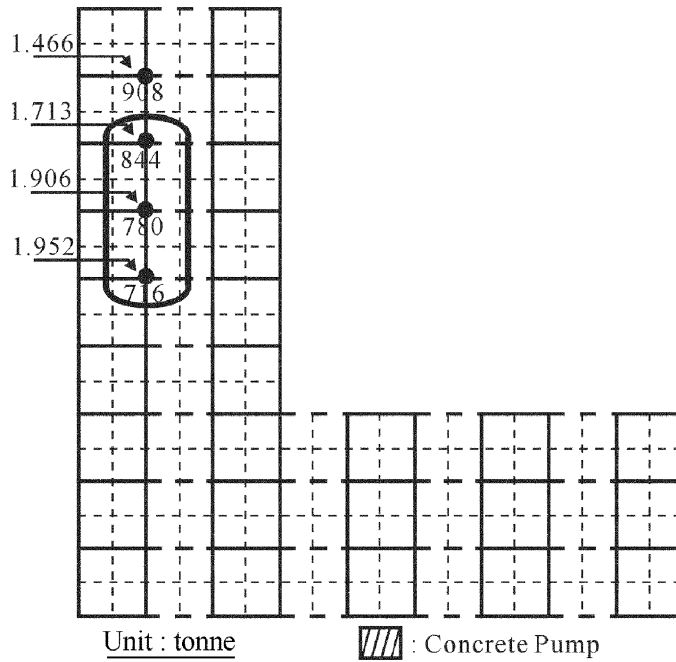


Fig. 18 Largest reaction force area of 6-bay *L* model under pattern load

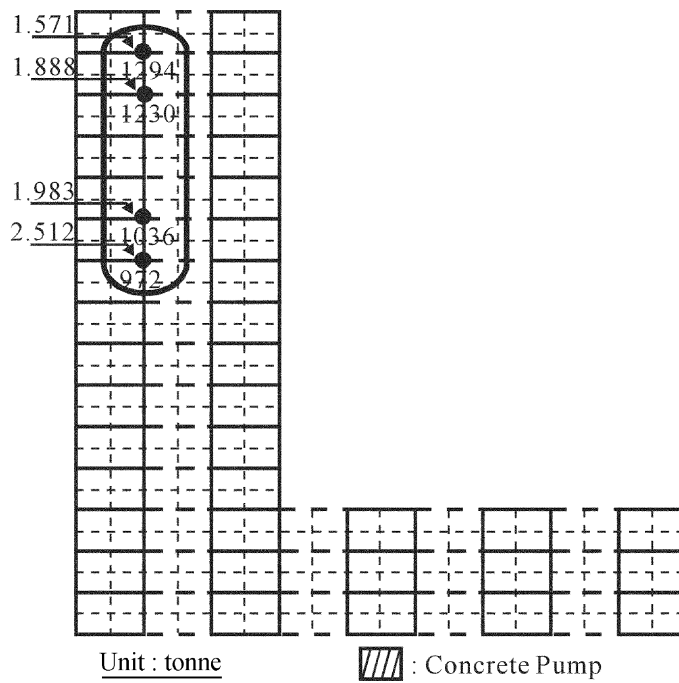


Fig. 19 Largest reaction force area of 12-bay *L* model under pattern load

Model U

The pattern load sequences of model *U* were surveyed from 25 concrete buildings in construction sites in Taiwan. As shown in Figs. 20 and 21, three and six bays from the bulge part of model *U* are investigated. The sequences of load patterns start from the left bulge part. The positions of these largest reaction forces are shown in Figs. 22 and 23. The positions of the largest reaction forces of these two types are mainly located on the left-hand side of the bulge part of model *U*. This corresponds to the location where the fresh concrete is placed. The position of largest reaction forces of model *U* is similar to that of model *L*. However, the region of model *L* has a greater spread than that of model *U*. This means that the positions of the largest reaction forces of model *U* are located on fewer positions than that of model *L*.

6.1.2 Comparison of largest reaction forces under sequential and uniform loads

This section investigates the values and positions of largest reaction forces excluded discussing the systems critical load of falsework. For the regions of largest reaction forces, the calculation under the sequential pattern load is complicate and time consuming compared with that under the uniform load. If the relationship between the sequential pattern load and uniform load are formulated, the complicated calculation by sequential pattern load can be directly substituted by simple uniform load in design. The sequential pattern load is based on the load type in Fig. 4. The following observations are based on models *R*, *L* and *U*.

Model R

Based on the observation of the uniform load, types (I) and (II) of model *R* have the same result after placing the uniform load on the formwork. Fig. 24 shows a three dimensional distribution of reaction forces of the system after pattern loading has been imposed completely, i.e., using the uniform load. From the contour map in Fig. 24, the contour lines exhibit the maximum reaction forces symmetrically.

Fig. 25 shows the largest reaction force with numbers adopted from the contour map in Fig. 24. As shown from Fig. 25, the largest reaction forces withdraw in the inner closed strip region from the outside edge. Positions 44, 76, 545 and 577 referred to the analysis nodes have the maximum reaction force in the system. The area with slash lines on the closed strip region shows the region of largest reaction forces in model *R*. This distribution of largest reaction forces is similar to that described by Peng *et al.* (1996c).

Fig. 26 shows the combined result by Fig. 25 under uniform load and Fig. 7 under sequential pattern load. In Fig. 26, the solid symbol “●” presents the positions of largest reaction forces from sequential pattern load and the hollow symbol “○” from uniform loads. The regions of largest reaction forces of the two cases are similar and are located near the lower left corner of the formwork.

Model L

Figs. 27, 28 and 29 show the analysis results of three, six and twelve bays of model *L* under uniform load. The three-dimensional distribution and contour map of reaction forces are shown in Figs. 27, 28 and 29. Figs. 30, 31 and 32 show the combination of the largest reaction force distribution of uniform load in Figs. 27, 28 and 29 and of sequential pattern load in Figs. 17, 18 and 19. As can be seen from these Figures, the overlay positions of the largest reaction forces for the two conditions are located at the extended bulge part of model *L* and from the middle to the top edge of the extended bulge part. Although the trend of the three cases is similar, the positions

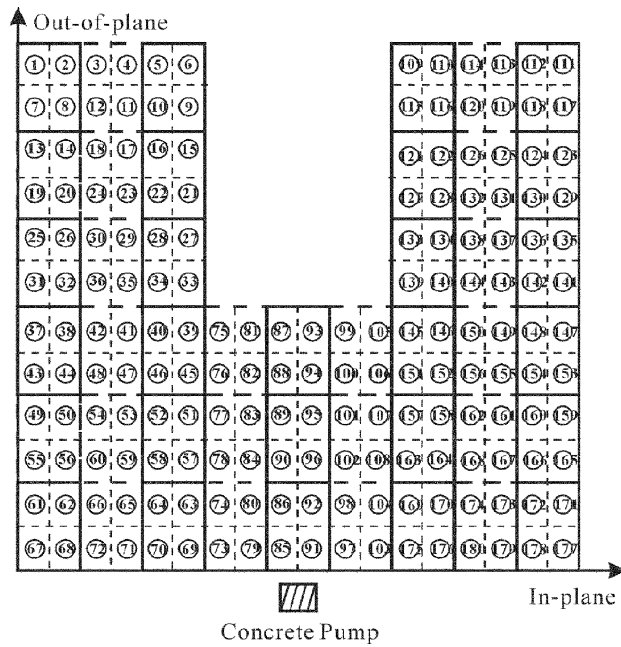


Fig. 20 Load pattern of 3-bay *U* model from survey of construction sites

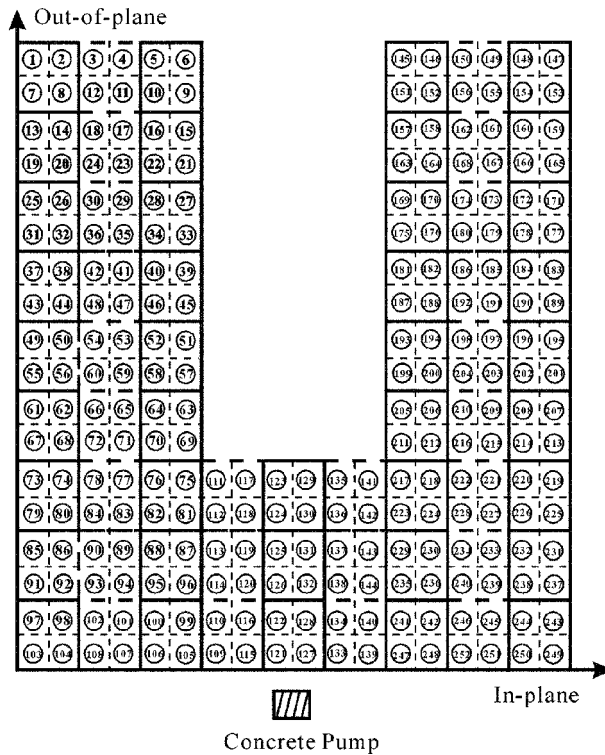


Fig. 21 Load pattern of 6-bay Model *U* from survey of construction sites

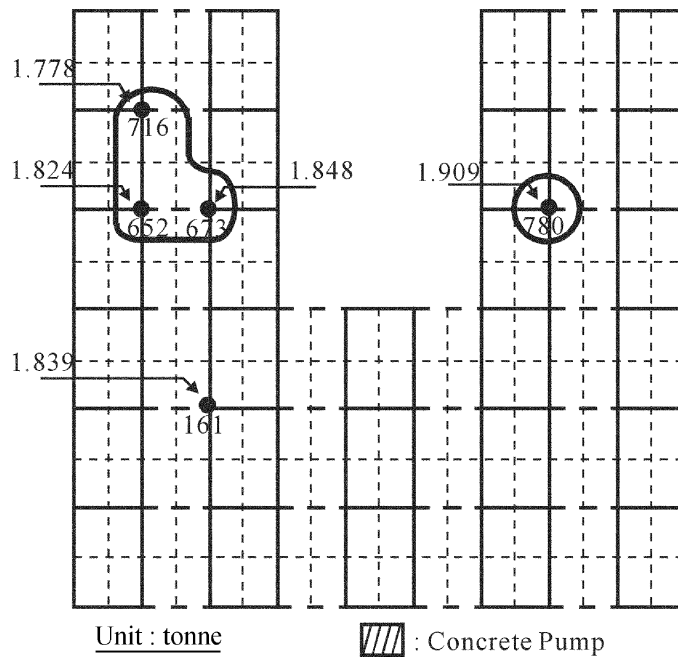


Fig. 22 Largest reaction forces of 3-bay model *U* under pattern load

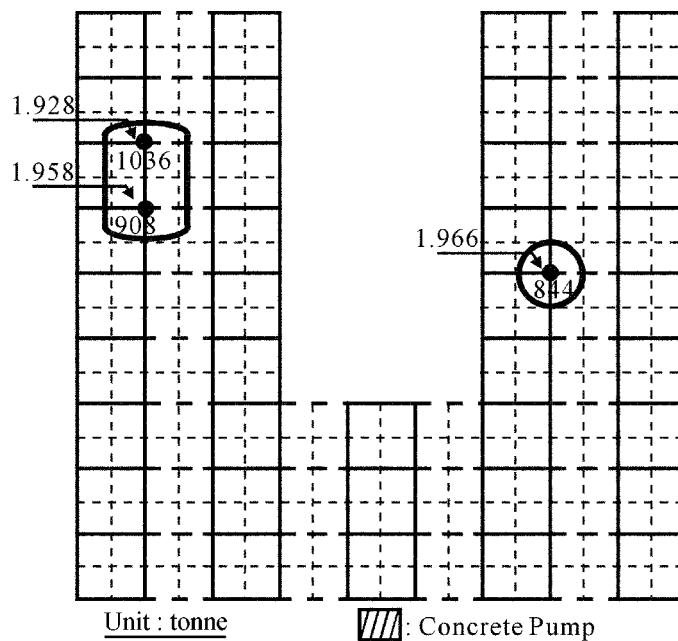


Fig. 23 Largest reaction force area of 6-bay *U* model under pattern load

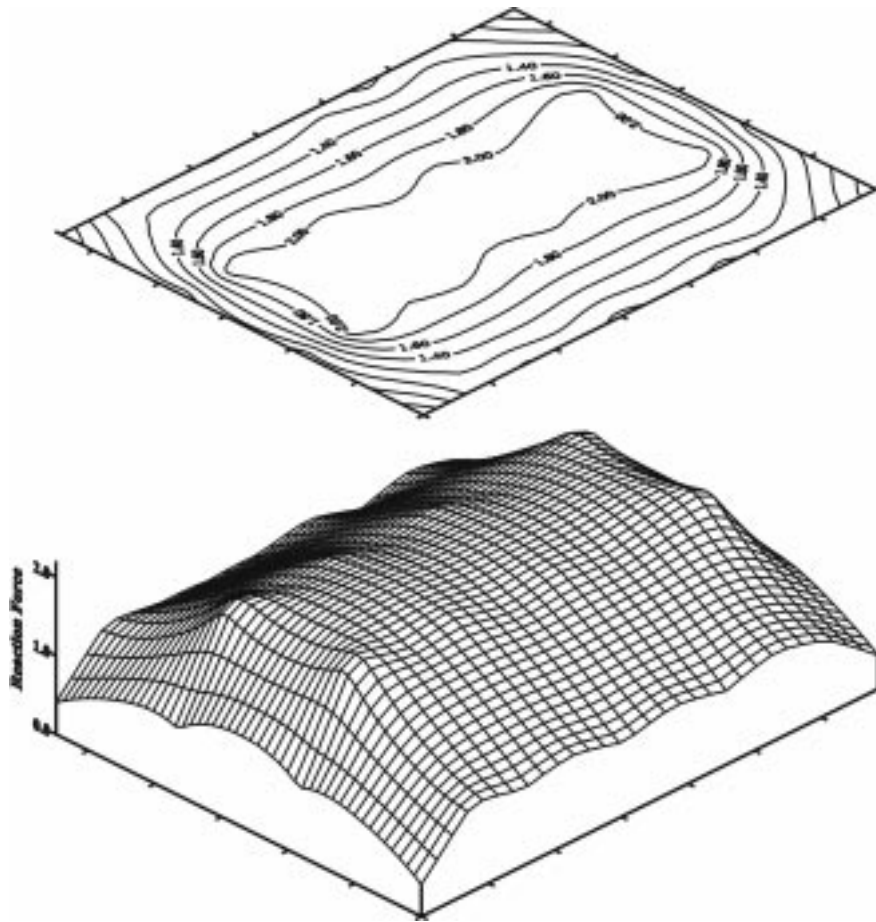


Fig. 24 Tubular axial force of *R* models (I) & (II) under uniform load

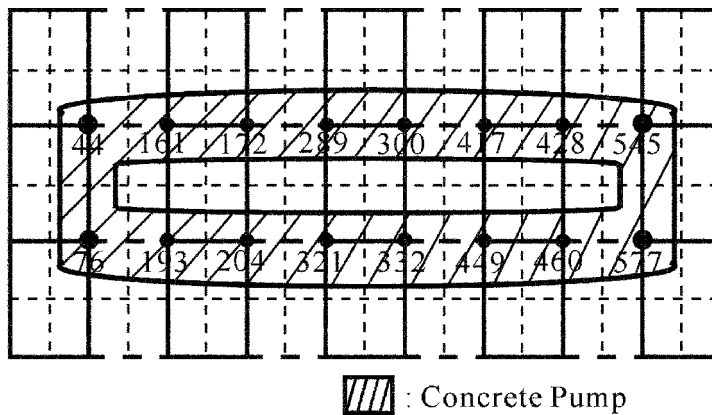


Fig. 25 Comparison of largest reaction forces of rectangle models (I) & (II) after load

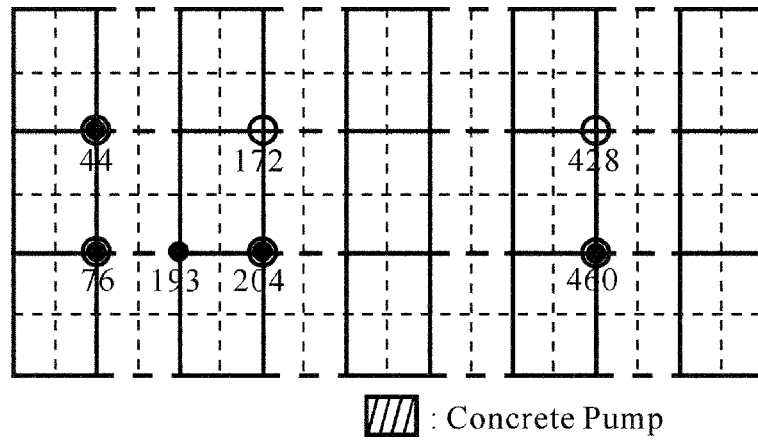


Fig. 26 Comparison of largest reaction force positions of rectangle models (I) & (II) after pattern and uniform loads

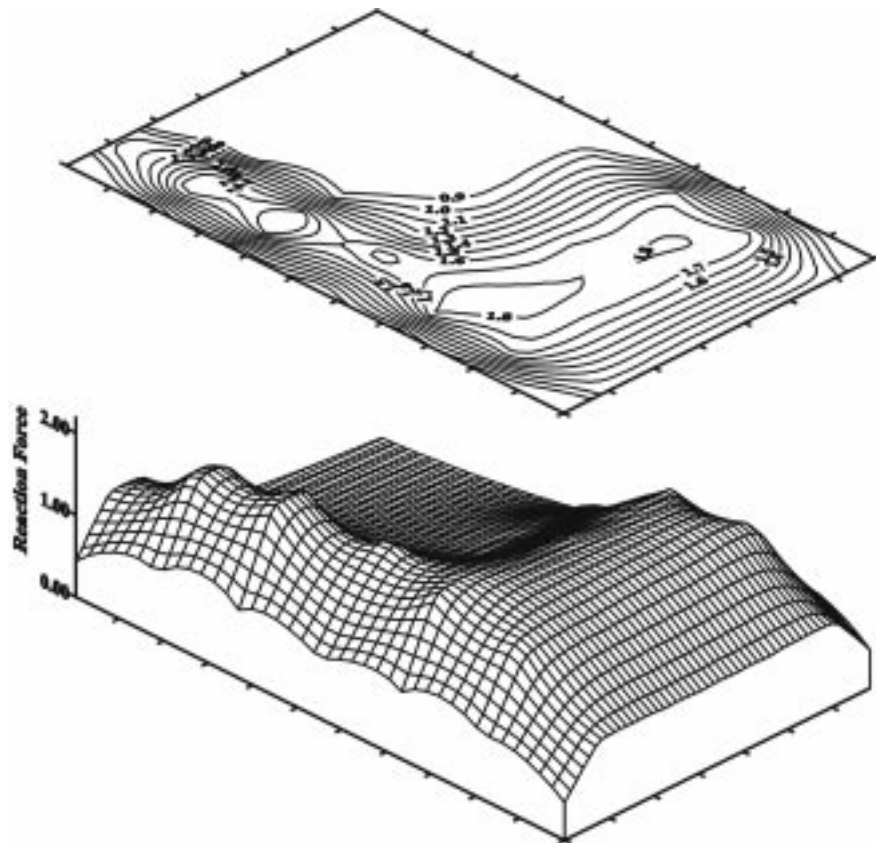


Fig. 27 Tubular axial force distribution of 3-bay *L* model under uniform load

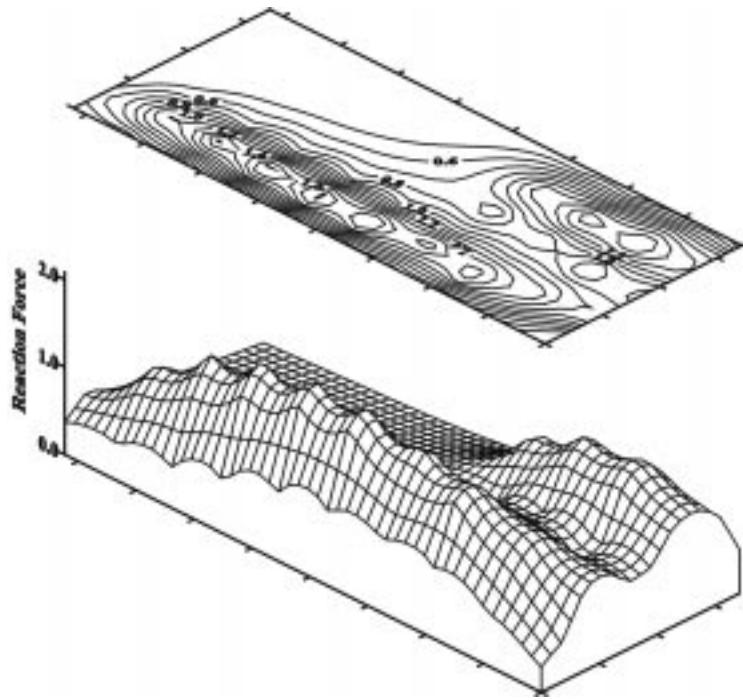


Fig. 28 Tubular axial force distribution of 6-bay L model under uniform load

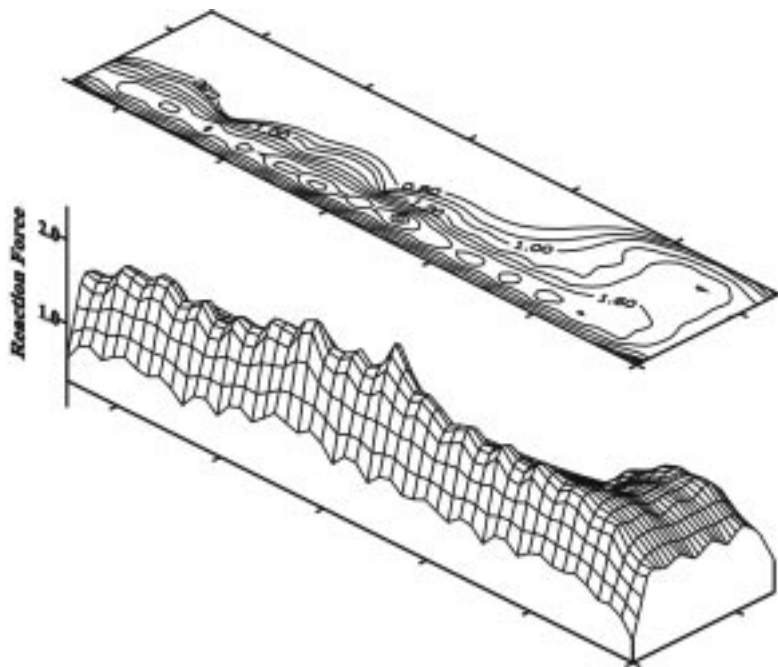


Fig. 29 Tubular axial force distribution of 12-bay L model under uniform load

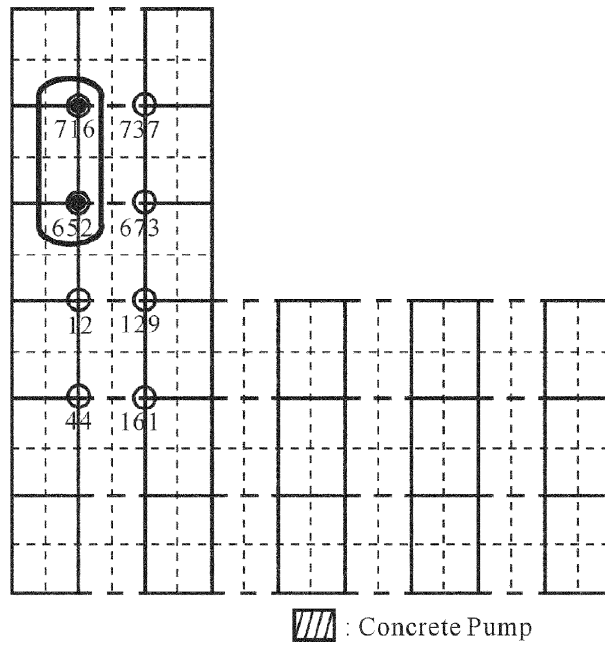


Fig. 30 Comparison of largest reaction force positions of 3-bay *L* model under pattern and uniform loads

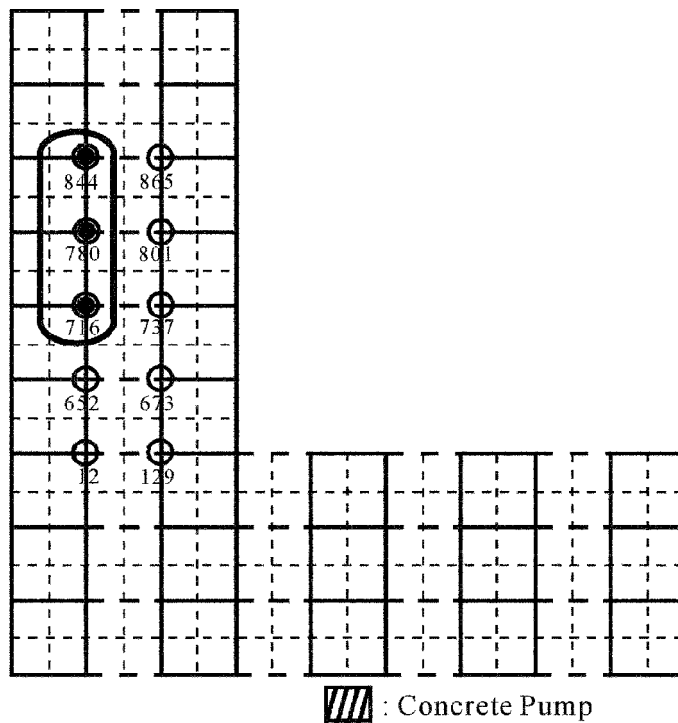


Fig. 31 Comparison of largest reaction force positions of 6-bay *L* model under pattern and uniform loads

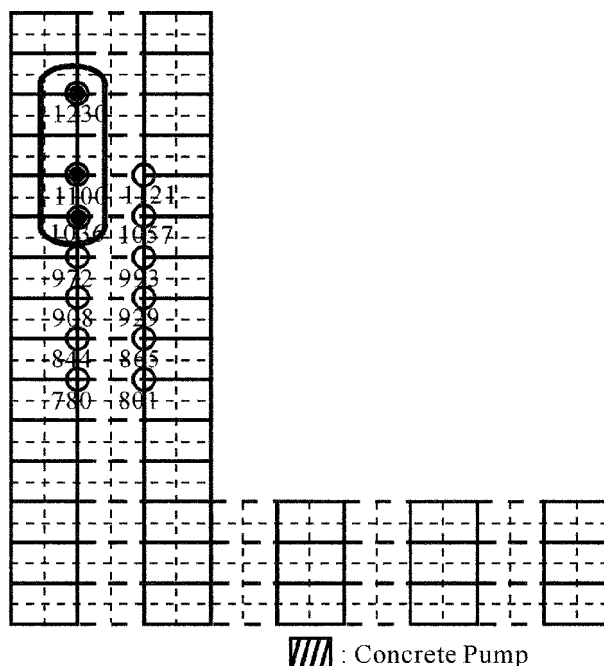


Fig. 32 Comparison of largest reaction force positions of 12-bay *L* model after pattern and uniform loads

calculated by the uniform loads are still different from those calculated by sequential pattern loads.

As described for the three bays of model *L*, the regions of largest reaction forces under uniform loads are similar to those under sequential pattern loads. However, the area under the sequential pattern load is larger than that under the uniform load. In design, the calculation of the uniform load is not conservative when compared with the sequential pattern load. Engineers should, therefore, be cautious when using the uniform load to predict the regions of largest reaction forces of model *L* in construction practice.

Model *U*

As previously mentioned, the three and six bays of model *U* under uniform loads are investigated on the basis of the survey study results of construction sites in Taiwan. Figs. 33 and 34 show the distribution of reaction forces for the cases of three and six bays. The two Figures present the three dimensional distributions of reaction forces and their contour maps.

Figs. 35 and 36 show the combinations of the largest reaction force distributions of uniform loads in Figs. 33 and 34 and of sequential pattern loads in Figs. 22 and 23 respectively. In these Figures, the definition of the symbols is the same as that of model *L*. As shown in Figs. 35 and 36 for the uniform loads, the two cases have similar distribution of largest reaction forces. The largest reaction forces of two cases under uniform loads are symmetrically distributed on the two extended bulge parts of model *U*. However, the distribution area of model *U* is larger than that of model *L*. In addition, the distribution of the uniform load is not similar to that of the sequential pattern load, concentrated on single extended bulge part shown in Figs. 22 and 23. Designers may, therefore, cautiously utilize the uniform load instead of the sequential pattern load to calculate the region of largest reaction forces for model *U* in design.

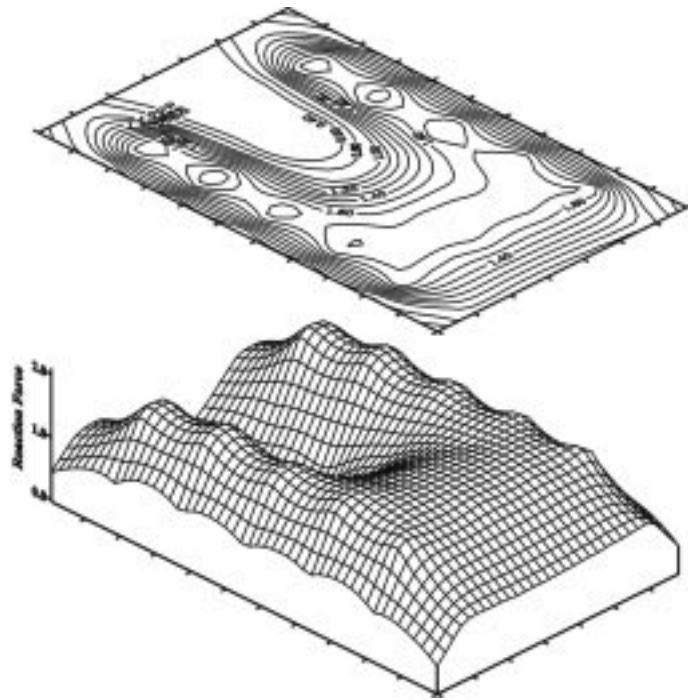


Fig. 33 Tubular axial force distribution of 3-bay *U* model under uniform load

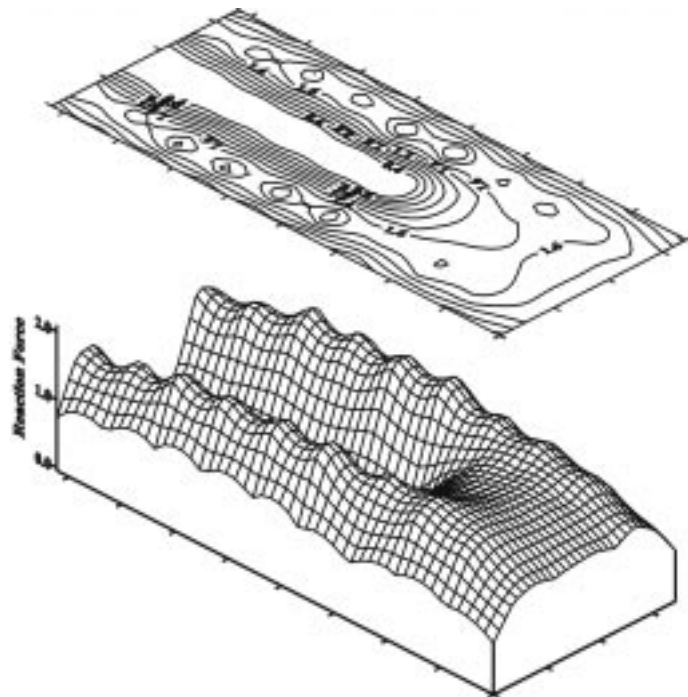


Fig. 34 Tubular axial force distribution of 6-bay *U* model under uniform load

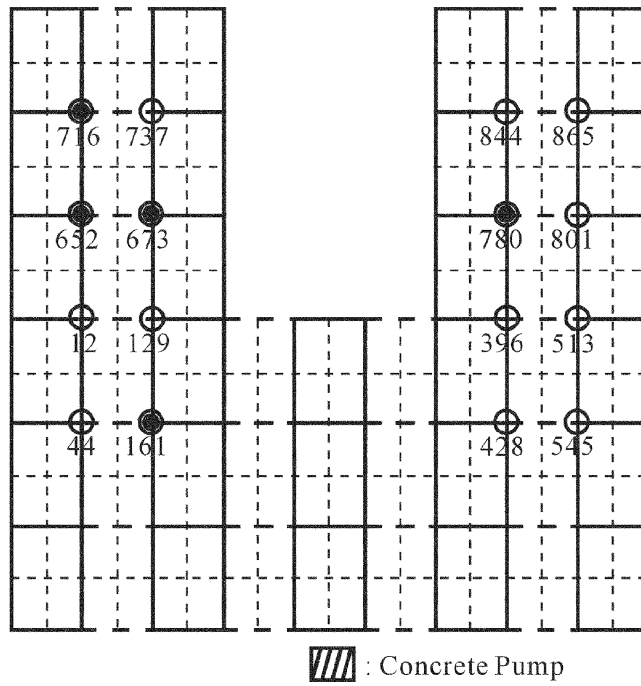


Fig. 35 Comparison of largest reaction force positions of 3-bay *U* model after pattern and uniform loads

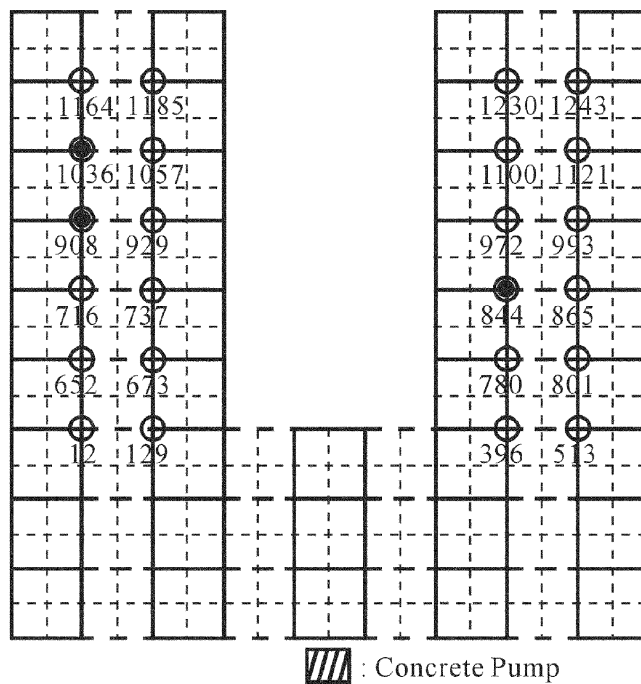


Fig. 36 Comparison of largest reaction force positions of 6-bay *U* model after pattern and uniform loads

6.2 Warning-system plan based on reaction forces

The warning-system of the falsework has two typical questions: (1) a suitable measuring index and (2) the location of setting-up the warning-system. Since the collapse of the falsework generally involves structural instability, the load as measured index is better than the lateral deformation. However, for a large area of formwork prepared for casting fresh concrete, the locations to install load-measured devices, such as load cells, are parameters for the warning-systems in construction. This study provides possible regions of largest reaction forces for the second problem of setting up of an on-site warning-system device.

As mentioned above for models *R*, *L* and *U* with the specific pattern load sequences as described by Peng *et al.* (2000), this study proposes the locations of the warning-system in the regions of largest reaction forces. These proposed regions can be established by above analyses with the following provision for the warning-system.

Model *R*

As shown in Fig. 37(A), an *L*-type region is suitable for the warning-system of model *R*. Based on Figs. 7 and 13, the preferred point of the warning-system device is located near the left-hand bottom corner and the concrete pump shown in Fig. 37(A). The warning-system device is installed from point A to the two arrow directions. Two rows of shores should be included in the rightward and upward directions.

Model *L*

The preferred point of the warning-system device is placed at the middle of the extended bulge part of model *L* as shown in Figs. 17, 18 and 19. As shown in Fig. 37(B), point A is the reference point. In fact, the region for the warning-system device can be located near the vicinity of point A to the extend bulge part of model *L* in Fig. 37(B).

Model *U*

Similar to model *L*, the preferred point of the warning-system device is located at the middle of the left extended bulge part of model *U* based on Figs. 22 and 23. Point A is the reference point in Fig. 37(C). The warning-system device can be set up near the vicinity of point A to the region of the extended bulge part by the arrow direction.

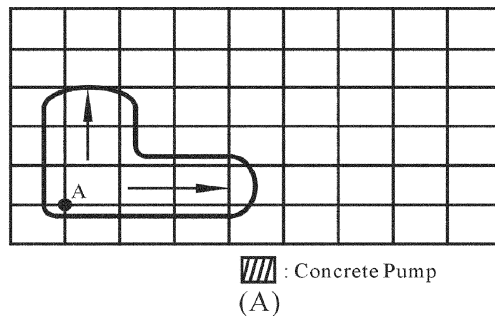


Fig. 37 Placement recommendation of *R*, *L* and *U* models for alert-system

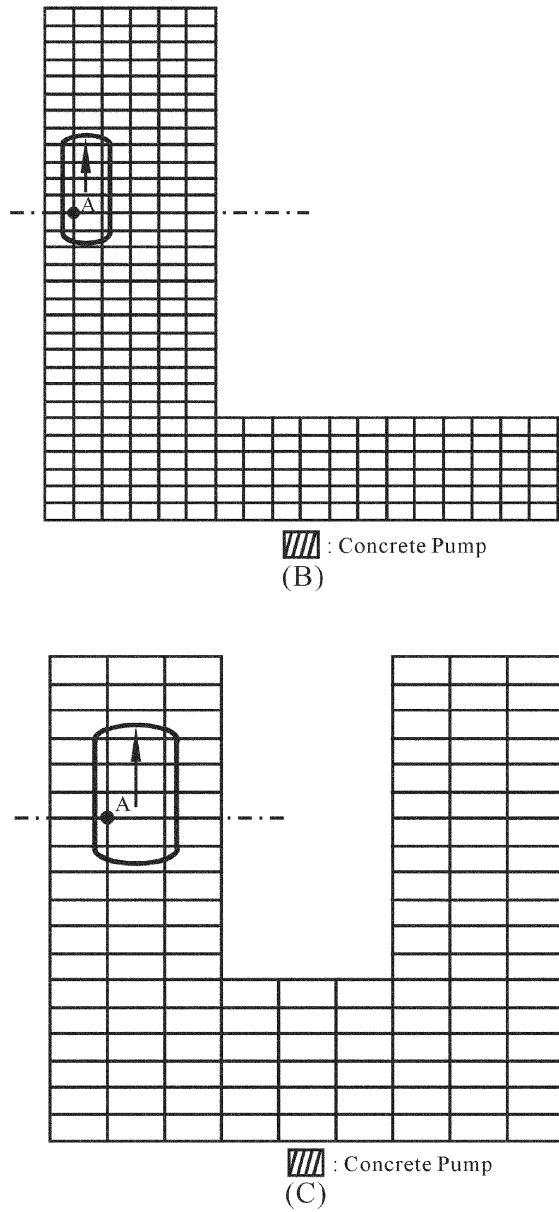


Fig. 37 Placement recommendation of *R*, *L* and *U* models for alert-system

7. Conclusions

1. The critical load and positions of largest reaction forces of modular falsework system were verified by an outdoor large full-scale loading test. The analysis is, therefore, considered reliable and acceptable.

2. The system critical loads of the modular falsework system under the sequential pattern and uniform loads are almost identical. Engineers can therefore consider using the uniform load instead of the sequential pattern load to calculate the system critical load in practical design.
3. The regions of largest reaction forces of models R , L and U are different under sequential pattern loads, respectively. However, models L and U with different bays have similar distributions of largest reaction forces.
4. The regions of largest reaction forces of models L and U under uniform loads are apparently larger than those under sequential pattern loads. Using uniform load to predict the region is unconservative in design. Therefore, the uniform load is not a suitable substitute for sequential pattern loads to predict the regions of largest reaction forces.
5. For the warning-system plan, the installed position of the warning-system device for model R is located near the second row of shores behind the concrete pump, the middle to the edge of the extended bulge part for model L far from the concrete pump, and the middle to the edge of the left extended bulge part for model U as shown in Fig. 37.

Acknowledgements

The authors would like to acknowledge Professor T. Yen of the National Chung-Hsing University for his valuable comments. The financial support from the National Science Council (NSC 87-2211-E-324-002) in Taiwan and from the Hong Kong Polytechnic University (BQQ 465) is greatly appreciated.

References

- Chan, S.L. (1988), "Geometric and material nonlinear analysis of beam-columns and frames using the minimum residual displacement method", *Int. J. Numer. Meth. Eng.*, **26**, 2657-2669.
- Chan, S.L. and Zhou, Z.H. (1994), "A pointwise equilibrium polynomial (PEP) element for nonlinear analysis of frame", *ASCE J. Struct. Eng.*, **120**(6), June, 1703-1717.
- Council of Labor Affairs. (1997), "Investigations of construction accidents: 1993-1995", (IOSH86-03). *Research Rep.*, Taipei, Taiwan, 898pp. (in Chinese).
- Hadipriono, F.C. and Wang, H.K. (1986), "Analysis of causes of formwork failures in concrete structures", *ASCE J. Construction Engineering and Management*, **112**(1), March, 112-121.
- Huang, Y.L., Chen, H.J., Rosowsky, D.V. and Kao, Y.G. (2000), "Load-carrying capacities and failure modes of scaffold-shoring systems, Part I: Modeling and experiments", *Structural Engineering and Mechanics*, **10**(1), 53-66.
- Jirsa, J.O., Sozen, M.A. and Siess, C.P. (1969), "Pattern loadings on reinforced concrete floor slabs", *J. Struct. Div.*, ASCE, **96**(ST6), June, 1117-1137.
- Jofriet, J.C. and McNeice, G.M. (1971), "Pattern loading on reinforced concrete flat plates", *Proc.*, ACI, **68**, December, 968-972.
- Peng, J.L., Pan, A.D., Rosowsky, D.V., Chen, W.F., Yen, T., and Chan, S.L. (1996a), "High clearance scaffold systems during construction-I. Structural modelling and modes of failure", *Eng. Struct.*, **18**(3), 247-257.
- Peng, J.L., Rosowsky, D.V., Pan, A.D., Chen, W.F., Chan, S.L. and Yen, T. (1996b), "High clearance scaffold systems during construction-II. Structural analysis and development of design guidelines", *Eng. Struct.*, **18**(3), 258-267.
- Peng, J.L., Rosowsky, D.V., Pan, A.D., Chen, W.F., Chan, S.L. and Yen, T. (1996c), "Analysis of concrete placement load effects using influence surfaces", *ACI Struct. J.*, **93**(2), March-April, 180-186.

- Peng, J.L., Wu, C.L. and Huang, P.S. (2000), "Investigation of horizontal force and pattern load placing of fresh concrete", (in Chinese) *Proc. the 5th Nat. Conf. on Structural Engineering*, Taichung, Taiwan, **2**, 1087-1094.
- Peng, J.L., Yen, T., Lin, I., Wu, K.L. and Chen, W.F. (1997), "Performance of scaffold frame shoring under pattern loads and load paths", *ASCE J. Construction Engineering and Management*, **123**(2), 138-145.
- Rosowsky, D.V., Huang, Y.L., Chen, W.F. and Yen, T. (1994a), "Modeling concrete placement loads during construction", *Structural Engineering Review*, **6**(2), 71-84.
- Rosowsky, D., Huston, D., Fuhr, P. and Chen, W. (1994b), "Measuring formwork loads during construction", *Concrete International*, ACI, **16**(11), 21-25.
- Yen, T., Huang, Y.L., Peng, J.L., Chen, H.J., Lin, I. and Liu, T.M. (2000), "Technology of construction safety for falsework of higher clearance and large concrete placing area", (in Chinese) *Research Report - IOSH89-S121*, Council of Labor Affairs, Taipei, Taiwan, 245pp.

Conversion Factors

To convert	To	Multiply by
tonne	kN	9.807